Journal of Magnetism and Its Applications, 2 (2) 2022, 23-26

http://www.jourmag.org/index.php/jma

Journal of Magnetism and Its Applications

Received September 10th 2022; received in revised October 19th 2022; accepted November 7th 2022

Research articles

Crystal Structures and Morphology of $Ni_{0.4}Zn_{0.6-x}Co_xFe_2O_4$ Magnetic Nanoparticles: Influence of Co Doping

Joko Utomo[1]*, Nur Elma Ayu Wahyuni[1], Nuviya illa Muthi Aturroifah[1], Sayyidati Zuhroh[1], Ade Siyanti Nurul Hidayah[1], Adulsman Sukkaew[2]

[1]Department of Physics, Faculty of Mathematics and Natural Sciences, Universitas Negeri Malang, Malang, 65145, Indonesia
[2]Department of Renewable Energy Technology, Faculty of Science Technology and Agriculture, Yala Rajabhat University, Satang Sub-district, Muang District, 95000, Thailand

Article info

Keywords:
Ferrite
$Ni_{0.4}Zn_{0.6-x}Co_xFe_2O_4$
Octahedral
Tetrahedral
Co doping

Abstract

The objective of this research is to investigate the crystal structures and morphology of $Ni_{0.4}Zn_{0.6-x}Co_xFe_2O_4$ magnetic nanoparticles. The samples had been successfully obtained by coprecipitation technique followed by an annealing temperature of 600 °C. The influence of Co doping (x = 0.2 - 0.5) on crystal structures, morphological properties, and functional groups was studied. To begin with, based on the XRD results, all samples were polycrystalline with the spinel cubic structure having a remarkable plane orientation of (311). Moreover, the crystallinity degree of samples experienced a downward performance by the increase of co doping, in which the $Ni_{0.4}Zn_{0.6-x}Co_xFe_2O_4$ magnetic nanoparticles at x= 0.5 had the lowest crystallinity degree. Regarding the TEM characterization, the $Ni_{0.4}Zn_{0.6-x}Co_xFe_2O_4$ magnetic nanoparticles at x=0.3 depicted the spherical shape having the average particle diameter of approximately 17.5 nm with slight agglomeration. The increase of Co content on $Ni_{0.4}Zn_{0.6-x}Co_xFe_2O_4$ causes the increase of particle size. Finally, the existence of functional groups was found at 453.27 cm^{-1} and 690.52 cm^{-1} occupied at octahedral and tetrahedral sites, respectively which confirmed the presence of spinel structure.

1. Introduction

The modification of new magnetic materials is always needed to obtain the best performance for desired applications. Spinel ferrites are the most fascinating type of magnetic materials to be studied because of their unique characteristics such as good electrical and magnetic characteristics[1, 2]. Because of that, they can be applied in wide range of applications such as converters, biomedical field, and microwave devices [2–4] The characteristics of spinel ferrites can be improved by some adjustments like modifying cation distribution at tetrahedral (A) and octahedral (B) sites, choosing preparation technique and giving annealing process after the powder of ferrites obtained [4, 5]. However, the most significant influence to enhance their properties is addition of dopants with the different types in the ferrites [6, 7].

Zinc nickel (Zn-Ni) ferrites are examples of the potential spinel ferrites used due to their high electrical resistivity, good saturation magnetization so that it is suitable for high-frequency applications such as transformers and inductors [8]. The structure of Zn-Ni ferrites is mixed spinel which Zn^{2+} and Fe^{3+} cations are normally occupied at tetrahedral (A) sites, while Zn^{2+} and the part of Fe^{3+} cations are occupied at octahedral (B) sites [9, 10]. Parvatheeswara et al [4] reported that the addition of Mn^{2+} ions in Zn-Ni ferrites obtained the saturation magnetization in a range of 37.18 – 68.40 emu/g and crystallite size about 29 – 38 nm. However, the research did not show the trend of the structural parameters and magnetic properties by dopant of Mn^{2+} [4]. This is essential to be considered because the specific applications need certain properties of materials, in case of Zn-Ni ferrites. Meanwhile, the previous research conducted by Utomo et al [11] investigated that Co^{2+} dopant in Co – Ni ferrites resulted in the enhancement of lattice parameter, maximum magnetization, and coercivity. However, the particle distribution of the samples is moderately agglomerated with low crystallinity degree due to no annealing treatment after powder obtained.

Among the various synthesis techniques, there are commonly techniques conducted to produce spinel ferrites such as coprecipitation [12], combustion reaction [13], citrate method [14], conventional ceramic [15]. In the present work, coprecipitation technique is chosen to produce $Ni_{0.4}Zn_{0.6-x}Co_xFe_2O_4$ (Ni – Zn – Co ferrites) because of their advantages such as low cost and the simplest way to produce spinel ferrites [16]. In this present work, Co^{2+} content has been doped in Zn-Ni ferrites with the composition of $Ni_{0.4}Zn_{0.6-x}Co_xFe_2O_4$ (x= 0.2, 0.3, 0.4, and 0.5) by coprecipitation method. The replacement of Co^{2+} to Zn^{2+} ions at octahedral and tetrahedral sites was studied to enhance their properties in structural parameters, morphology, and vibrational spectra of $Ni_{0.4}Zn_{0.6-x}Co_xFe_2O_4$ magnetic nanoparticles. Furthermore, the objective of this research is to investigate the crystal structures and morphology of $Ni_{0.4}Zn_{0.6-x}Co_xFe_2O_4$ magnetic nanoparticles by Co doping.

2. Experimental Method

The main raw materials used in this process were $NiCl_2.6H_2O$ (Sigma Aldrich, Germany), $ZnSO_4.7H_2O$ (Sigma Aldrich, Germany), $CoCl_2.6H_2O$ (Sigma Aldrich, Germany), and $FeCl_3.6H_2O$ (Sigma Aldrich, Germany). To begin with, the raw materials were dissolved together into a beaker glass and stirred by a magnetic stirrer with the fixed calculation of stoichiometric ratio for each material. The HCl was then added to the solution to accelerate the chemical reaction. In another stage, the solution of NaOH was made in 25 ml distilled water and stirred for 1 hour with the synthesis temperature of 90 °C. The next stage, the obtained ferrite solution was dropped gently into the NaOH solution while the stirring process was still processed. After 1 h, the precipitate was obtained and then washed for six times to diminish the remaining salt solution with the help of a permanent magnet. Afterwards, the product was dried into a furnace with the temperature of 90 °C. In the following step, the obtained powders were followed by giving annealing with high temperature of 600 °C. Finally, the final product was characterized by XRD Panalytical Xpert Pro, TEM JEOL JEM-1400, and FTIR spectrophotometer (IR Prestige-21, Shimadzu) to study respectively structural parameters, morphology, and vibrational spectra of $Ni_{0.4}Zn_{0.6-x}Co_xFe_2O_4$ (x= 0.2, 0.3, 0.4, and 0.5) magnetic nanoparticles.

*Corresponding author
Email: joko.utomo.fmipa@um.ac.id

DOI: 10.53533/JMA.v2i1.27

3. Results and Discussion

The structural parameters for all prepared samples have been investigated by XRD characterization. The XRD patterns of $Ni_{0.4}Zn_{0.6-x}Co_xFe_2O_4$ magnetic nanoparticles are portrayed in Figure 1. Based on Figure 1, the single phase is found for all samples (x=0.2 – 0.5) with no impurities from another phase. The miller indices obtained for all the prepared samples at (220), (311), (400), (422), (511), and (440) represent the spinel cubic structures with the group space of ferrite, namely *Fd3m*. This is in line with the data standard of JCPDS Number 22-1086 relating to the formation of single cubic phase [17] . Qualitatively, the sample at x = 0.5 has a lower crystallinity degree than other samples. The enhancement of Co content causes the diffraction angle shifted to the higher value that is related to the change of lattice parameter (a) and crystallite size (t). The crystallites size (t) of $Ni_{0.4}Zn_{0.6-x}Co_xFe_2O_4$ magnetic nanoparticles can be calculated by the following Scherrer's equation [18] :

$$t = \frac{0.9\,\lambda}{\beta \cos\theta} \quad (1)$$

where β is the FWHM of the peak intensity (311), λ is the wavelength of X-ray (1.5406 Å), and θ is the angle diffraction at (311) [19].

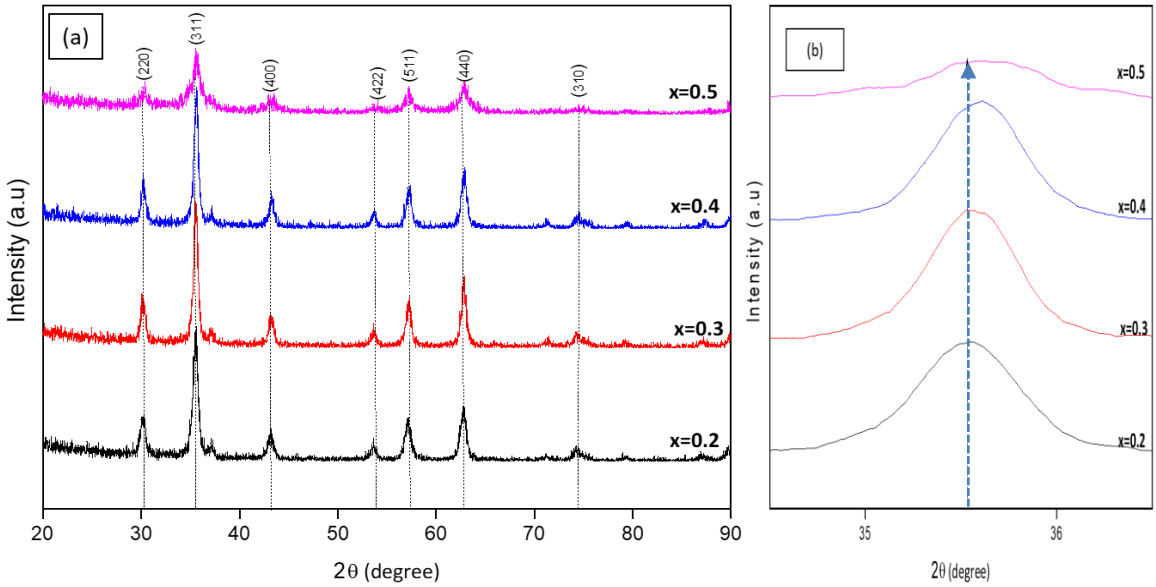

Fig. 1. (a) X-ray diffraction of $Ni_{0.4}Zn_{0.6-x}Co_xFe_2O_4$ magnetic nanoparticles and (b) the enlargement of the miller indices (311)

The detailed information about the structural parameters (crystallite size, lattice parameter, X-ray density, and strain) are shown in Table 1.

Table 1. The structural values of $Ni_{0.4}Zn_{0.6-x}Co_xFe_2O_4$ (x=0.2-0.5) magnetic nanoparticles

Ferrite composition	Crystallite size (nm)	Lattice parameter (Å)	X-ray density (× 10^3 kg/m^3)	Strain
$Ni_{0.4}Zn_{0.4}Co_{0.2}Fe_2O_4$	13.37	8.374	5.303	0.034
$Ni_{0.4}Zn_{0.3}Co_{0.3}Fe_2O_4$	15.79	8.367	5.316	0.028
$Ni_{0.4}Zn_{0.2}Co_{0.4}Fe_2O_4$	15.61	8.360	5.330	0.029
$Ni_{0.4}Zn_{0.1}Co_{0.5}Fe_2O_4$	16.73	8.353	5.343	0.027

According to Table 1, the lattice parameter is slightly decreased with the enhancement of Co fraction. This is attributed to the difference of atom radii of bivalent metal ions. The replacement of smaller Co (0.745 Å) ions for larger Zn (0.82 Å) ions results in lattice shrinkage which gives the decrease of lattice constant. In contrast, X-ray density is linearly inclined with the addition of Co content. This is attributed to the atomic weight of Co and Zn. In addition, it is also obtained that crystallite size is linearly increased starting from 13.37 nm (x=0.2) to 16.73 nm (x=0.5) with the addition of Co content. In contrast, the sample at x=0.4 possesses a slight decrease trend compared to others. This phenomenon is because the growing process of nanoparticle crystallites took place imperfectly and resulted in smaller size. The detailed variation of the crystallite size and lattice parameter with the addition of Co content is given in Figure 2.

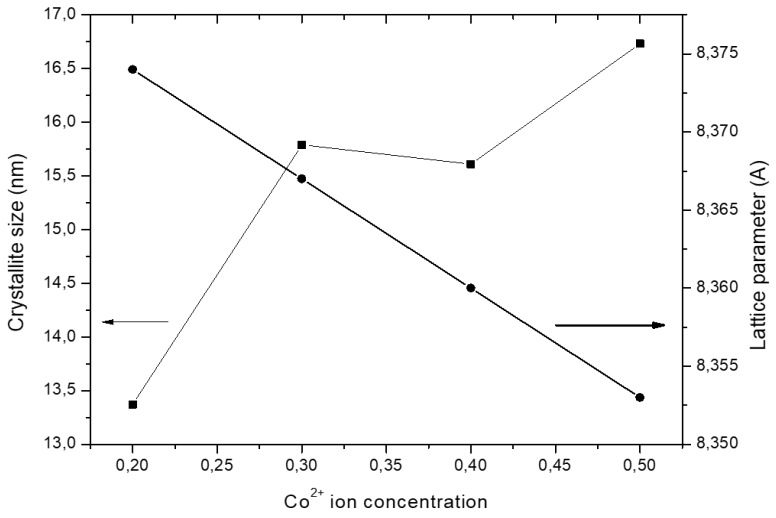

Fig. 2. Variation of the crystallite size and lattice parameter as a function of Co concentration

The morphology of annealed ferrites of $Ni_{0.4}Zn_{0.6-x}Co_xFe_2O_4$ magnetic nanoparticles at x = 0.1 and x = 0.3 is depicted in Figure 3. According to Figure 3, the particle distribution of $Ni_{0.4}Zn_{0.6-x}Co_xFe_2O_4$ at x = 0.1 is more agglomerated than x = 0.3. Nevertheless, these results are truly better than the samples without annealing after the coprecipitation process. The TEM results show that the majority shape of particles in all prepared samples is spherical. The average size of particles of $Ni_{0.4}Zn_{0.6-x}Co_xFe_2O_4$ magnetic nanoparticles at x = 0.1 and x = 0.3 are 15.5 nm and 17.5 nm, respectively which is increased with the addition of Co content.

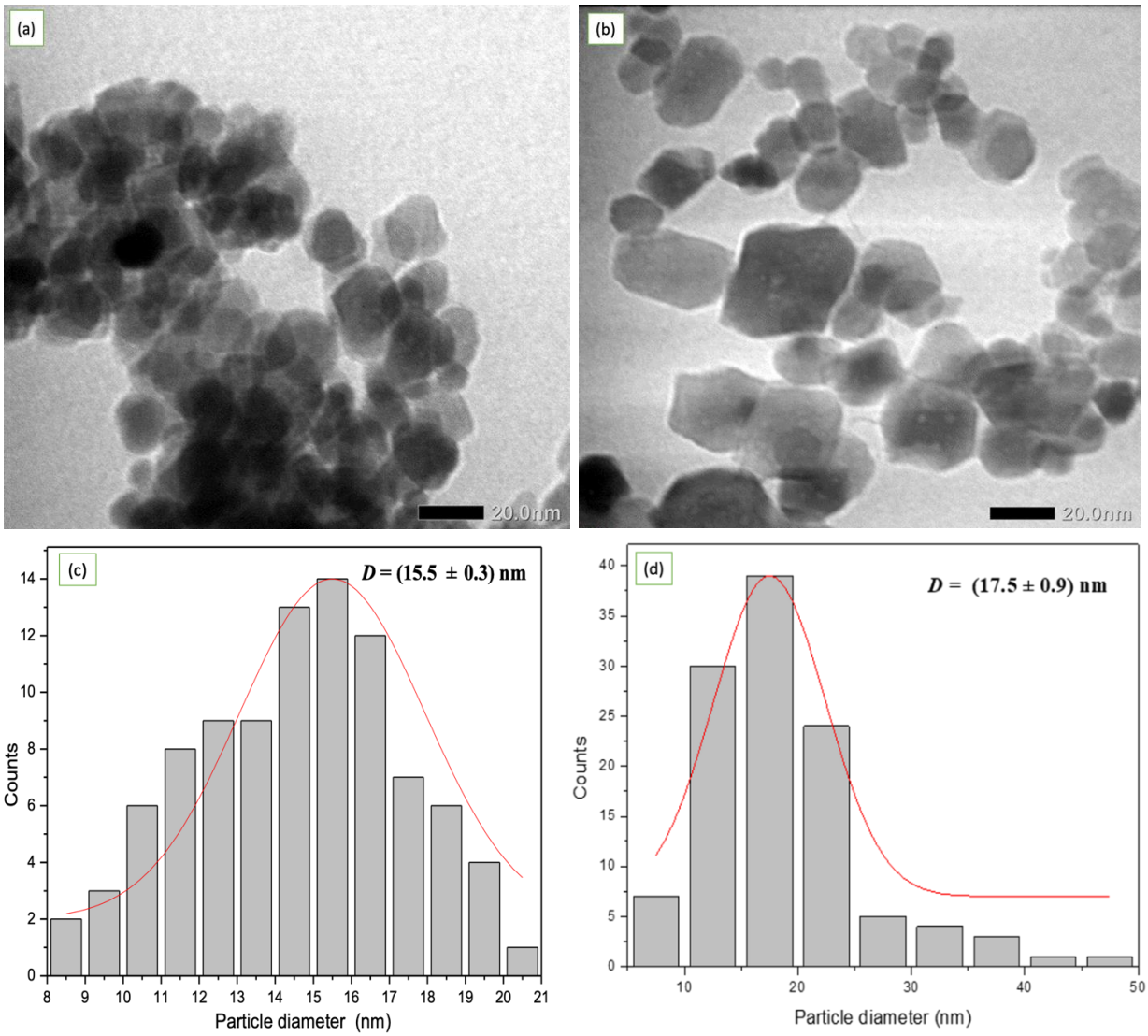

Fig. 3. The morphology of $Ni_{0.4}Zn_{0.6-x}Co_xFe_2O_4$ magnetic nanoparticles (a) x = 0.1; (b) x = 0.3, and the histogram of particle diameter of $Ni_{0.4}Zn_{0.6-x}Co_xFe_2O_4$ magnetic nanoparticles (c) x = 0.1; (d) x = 0.3

The vibrational spectra of $Ni_{0.4}Zn_{0.6-x}Co_xFe_2O_4$ magnetic nanoparticles are depicted in Figure 4. All prepared samples show the two prominent frequency bands which are about $\boldsymbol{\upsilon_1}$ (678.94 – 690.52) cm^{-1} and $\boldsymbol{\upsilon_2}$ (453.27 – 499.56) cm^{-1} located at tetrahedral and octahedral sites, respectively.

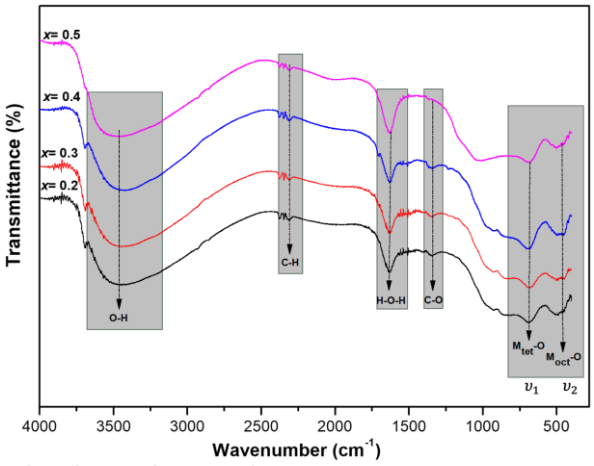

Fig. 4. The vibrational spectra of $Ni_{0.4}Zn_{0.6-x}Co_xFe_2O_4$ magnetic nanoparticles

The differences of frequency bands ($\boldsymbol{\upsilon_1}$ and $\boldsymbol{\upsilon_2}$) position are caused by the difference of ionic distance of Fe^{3+} – O^{2-} [20]. This indicates that all prepared samples are pure spinel phase and in good agreement with the XRD result. The detailed vibrational spectra ($\boldsymbol{\upsilon_1}$ and $\boldsymbol{\upsilon_2}$) of $Ni_{0.4}Zn_{0.6-x}Co_xFe_2O_4$ magnetic nanoparticles are shown in Table 2.

Table 2. Vibrational spectra ($\boldsymbol{\upsilon_1}$ and $\boldsymbol{\upsilon_2}$) of $Ni_{0.4}Zn_{0.6-x}Co_xFe_2O_4$ magnetic nanoparticles

Site	*x*			
	0.2	**0.3**	**0.4**	0.5
Tetrahedral	688.59	678.94	690.52	686.66
Octahedral	491.85	491.84	453.27	499.56

In addition, the presence of C – H stretching is because the sample reacts with CO_2 and H_2 gasses in the atmosphere during the preparation process such as the heating process in the furnace and testing samples with the FTIR instrument. Meanwhile, the vibration of hydroxyl groups such as O – H and H – O – H might be caused by the KBr compound during sample preparation for the FTIR test.

4. Conclusions

$Ni_{0.4}Zn_{0.6-x}Co_xFe_2O_4$ magnetic nanoparticles (x = 0.2 - 0.5) had been efficaciously prepared through coprecipitation method with the synthesis temperature of 90 °C. The X-ray diffraction pattern reveals the spinel cubic structures with the group space of *Fd3m*. In addition, the increase of Co content on $Ni_{0.4}Zn_{0.6-x}Co_xFe_2O_4$ causes the increase of crystallite size and x-ray density while the lattice parameter and strain were decreased. The TEM analysis shows the shape of particles is spherical with the average size of particles within 15.5 – 17.5 nm. Moreover, the increment of Co content causes the larger particles size. The FTIR investigation confirms that all prepared samples are pure spinel phase and in good agreement with the result of X-ray diffraction analysis.

Acknowledgments

The authors are thankful and grateful to PNBP KBK UM for providing financial support to conduct this work.

References

[1] Shoba M, Kaleemulla S, Krishnamoorthi C and Rao G V 2019 Effect of Er^{3+} substitution on structural and magnetic properties of narrow size distributed $ZnFe_{2-x}Er_xO_4$ nanoparticles *Appl. Phys. A Mater. Sci. Process.* 125 1–11
[2] De Oliveira V D, Rubinger R M, Da Silva M R, Oliveira A F, Rodrigues G and Dos Santos Ribeiro V A 2016 Magnetic and electrical properties of $Mn_xCu_{1-x}Fe_2O_4$ ferrite *Mater. Res.* 19 786–790
[3] Islam M N and Hossain A K M A 2019 Enhancement of Néel temperature and electrical resistivity of Mn-Ni-Zn ferrites by Gd^{3+} substitution *J. Mater. Res. Technol.* 8 208–216
[4] Parvatheeswara Rao B, Dhanalakshmi B, Ramesh S and Subba Rao P S V 2018 Cation distribution of Ni-Zn-Mn ferrite nanoparticles *J. Magn. Magn. Mater.* 456 444–450
[5] Utomo J, Agustina A K and Suharyadi E 2018 Annealing temperature effect on structural, vibrational and optical properties of $Co_{0.8}Ni_{0.2}Fe_2O_4$ nanoparticles *IOP Conf. Ser. Mater. Sci. Eng.* 432 1–7
[6] Norouzzadeh P, Mabhouti K, Golzan M M and Naderali R 2020 Consequence of Mn and Ni doping on structural, optical and magnetic characteristics of ZnO nanopowders: the Williamson–Hall method, the Kramers–Kronig approach and magnetic interactions *Appl. Phys. A Mater. Sci. Process.* 126 1–13
[7] Felhi R, Omrani H, Koubaa M, Koubaa W C and A. Cheikhrouhou 2018 Enhancement of magnetocaloric effect around room temperature in $Zn_{0.7}Ni_{0.3-x}Cu_xFe_2O_4$ ($0 \leq x \leq 0.2$) spinel ferrites *J. Alloy. Alloys Compd.* 758 237–246
[8] Kumar R, Kumar H, Singh R R and Barman P B 2016 Variation in magnetic and structural properties of Co-doped Ni–Zn ferrite nanoparticles: a different aspect *J. Sol-Gel Sci. Technol.* 78 566–575
[9] Mathew D S and Juang R S 2007 An overview of the structure and magnetism of spinel ferrite nanoparticles and their synthesis in microemulsions *Chem. Eng. J.* 129 51–65
[10] Prasad S A V, Deepty M, Ramesh P N, Prasad G, Srinivasaraoa K and Srinivas C 2018 Synthesis of MFe_2O_4 (M= Mg^{2+}, Zn^{2+}, Mn^{2+}) spinel ferrites and their structural, elastic and electron magnetic resonance properties *Ceram. Int* 44 10517-10524
[11] Utomo J, Agustina A K, Suharyadi E, Kato T and Iwata S 2018 Effect of Co concentration on crystal structures and magnetic properties of $Ni_{1-x}Co_xFe_2O_4$ nanoparticles synthesized by co-precipitation method 187 194 - 202
[12] Dey S, Dey S K, Majumder S, Poddar A, Dasgupta P, Banerjee S and Kumar S 2014 Superparamagnetic behavior of nanosized $Co_{0.2}Zn_{0.8}Fe_2O_4$ synthesized by a flow rate controlled chemical coprecipitation method *Phys. B Condens. Matter* 448 247–252
[13] Yadav R S, Havlica J, Hnatko M, Šajgalík P, Alexander C, Palou M, Bartoníčková E, Boháč M, Frajkorová F, Masilko J, Zmrzlý M, Kalina L, Hajdúchová M and Enev V 2015 Magnetic properties of $Co_{1-x}Zn_xFe_2O_4$ spinel ferrite nanoparticles synthesized by starch-assisted sol-gel autocombustion method and its ball milling *J. Magn. Magn. Mater.* 378 190–199
[14] Nawara A S and Mazen S A 2020 Synthesis, structural characterization, and magnetic properties of Ni–Zn nanoferrites substituted with different metal ions (Mn^{2+}, Co^{2+}, and Cu^{2+}) *J. Phys. Chem. Solids* 109620
[15] Stergiou C 2016 Microstructure and Electromagnetic Properties of Ni-Zn-Co Ferrite up to 20 GHz *Adv in Mat Sci and Eng* 1-7
[16] Irfan S, Nabi M A, Jamil Y, and Amin N 2014 Synthesis of $Mn_{1-x}Zn_xFe_2O_4$ ferrite powder by co- precipitation method Synthesis of $Mn_{1-x}Zn_xFe_2O_4$ ferrite powder by co-precipitation method *IOP Conf. Ser.: Mater. Sci. Eng.* 60 012048
[17] Sharma D and Khare N 2016 Tailoring the optical bandgap and magnetization of cobalt ferrite thin films through controlled zinc doping *AIP Adv.* 6 085005
[18] Kumar A L K 2015 Effects on structural , optical , and magnetic properties of pure and Sr-substituted $MgFe_2O_4$ nanoparticles at different calcination temperatures *Appl. Nanosci.* 6 629–639
[19] Tirupanyam B V., Srinivas C, Meena S S, Yusuf S M, Satish Kumar A, Sastry D L and Seshubai V 2015 Investigation of structural and magnetic properties of co-precipitated Mn-Ni ferrite nanoparticles in the presence of α-Fe_2O_3 phase *J. Magn. Magn. Mater.* 392 101–106
[20] Khan S B, Irfan S and Lee S L 2019 Influence of Zn^{+2} doping on ni-based nanoferrites; ($Ni_{1-x}Zn_xFe_2O_4$) *Nanomaterials* 9 1-17